ESS 312 Notes on the Origin of the Elements*

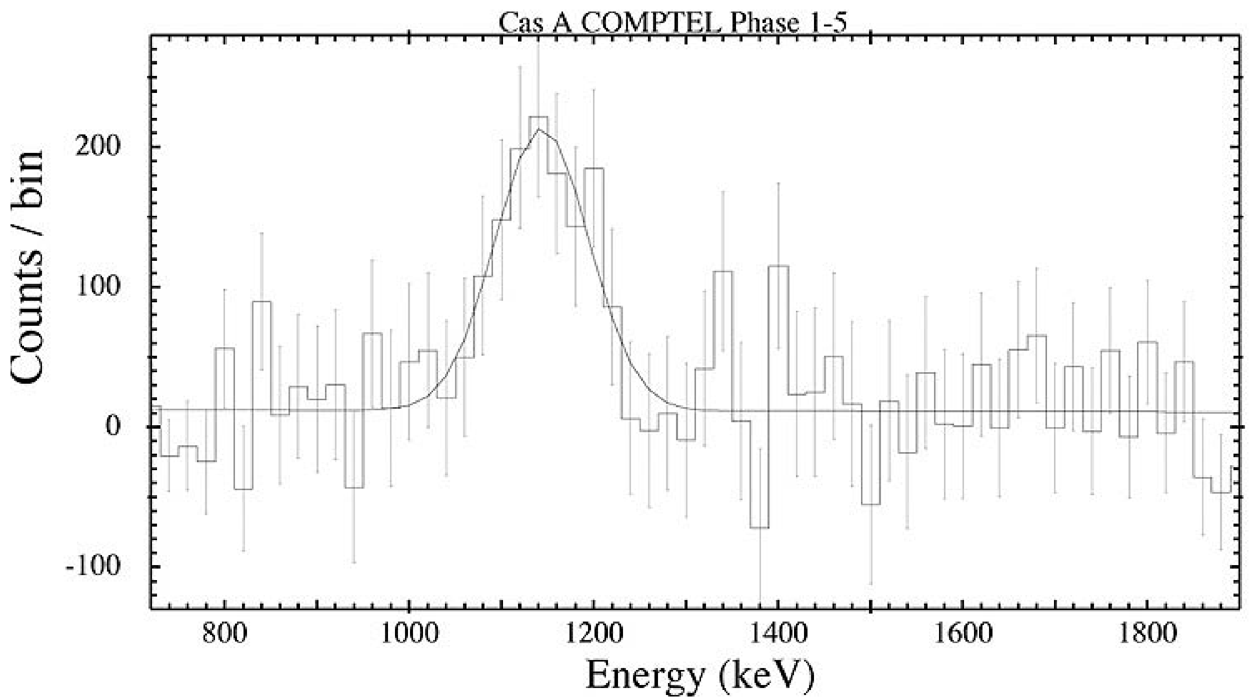

- Astronomical gamma ray emission from freshly created ^{44}Ti ($t_{1/2} = 47$ yr)

*Interest only - material will not be on the final exam

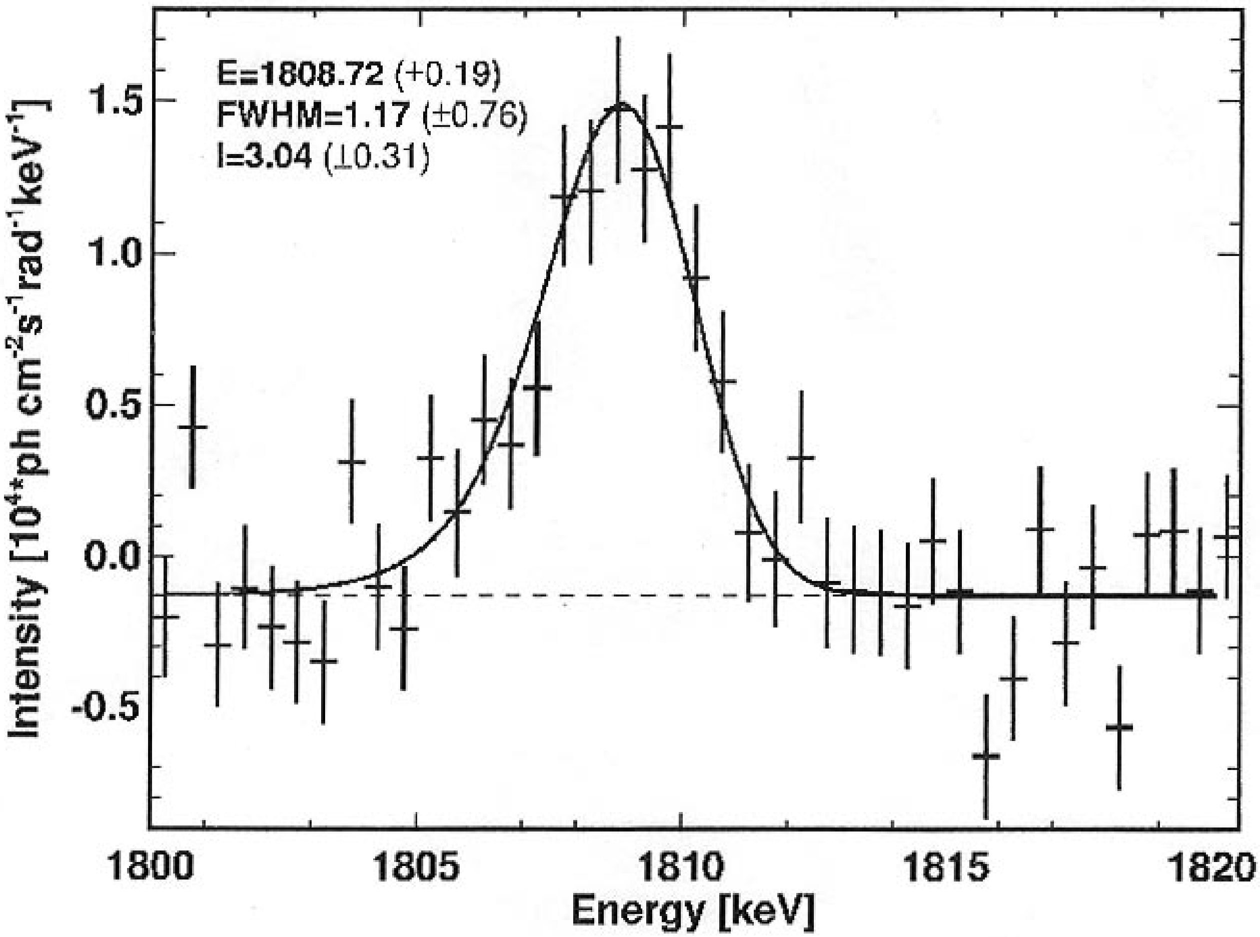

- Similarly - gamma ray emission from ^{26}Al ($t_{1/2} = 0.7$ Myr)

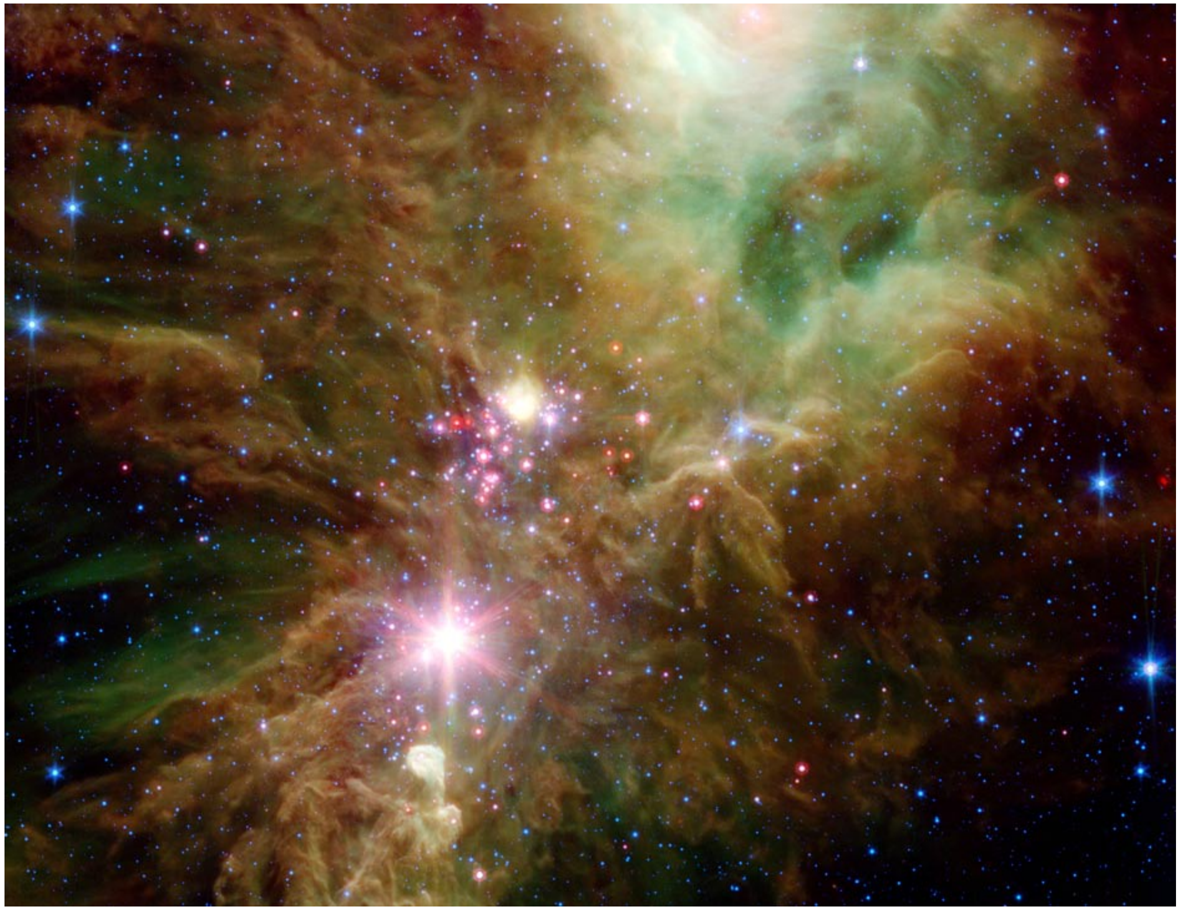

- Christmas Tree Nebula, example of a gas and dust-rich region where stars form

- Supernova 1987A, Large Magellanic Cloud. Composite of photos taken 7, 9 and 10 years after the explosion, showing ring of ejected debris expanding into surrounding gas cloud (Hubble ST; http://www.nasaimages.org).

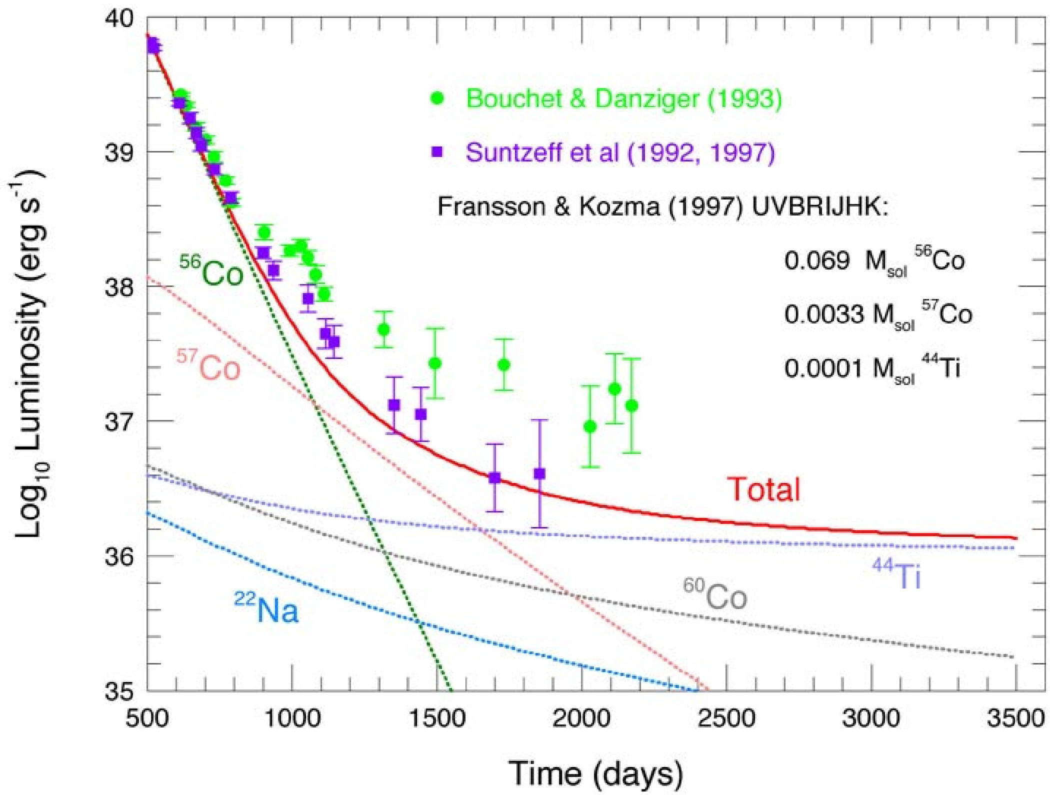

- Luminosity of SN1987A is sustained by decay of newly-formed radionuclides. Note the amounts - for Co-56 (which will decay to stable Fe-56) that's 23,000 x the mass of Earth!

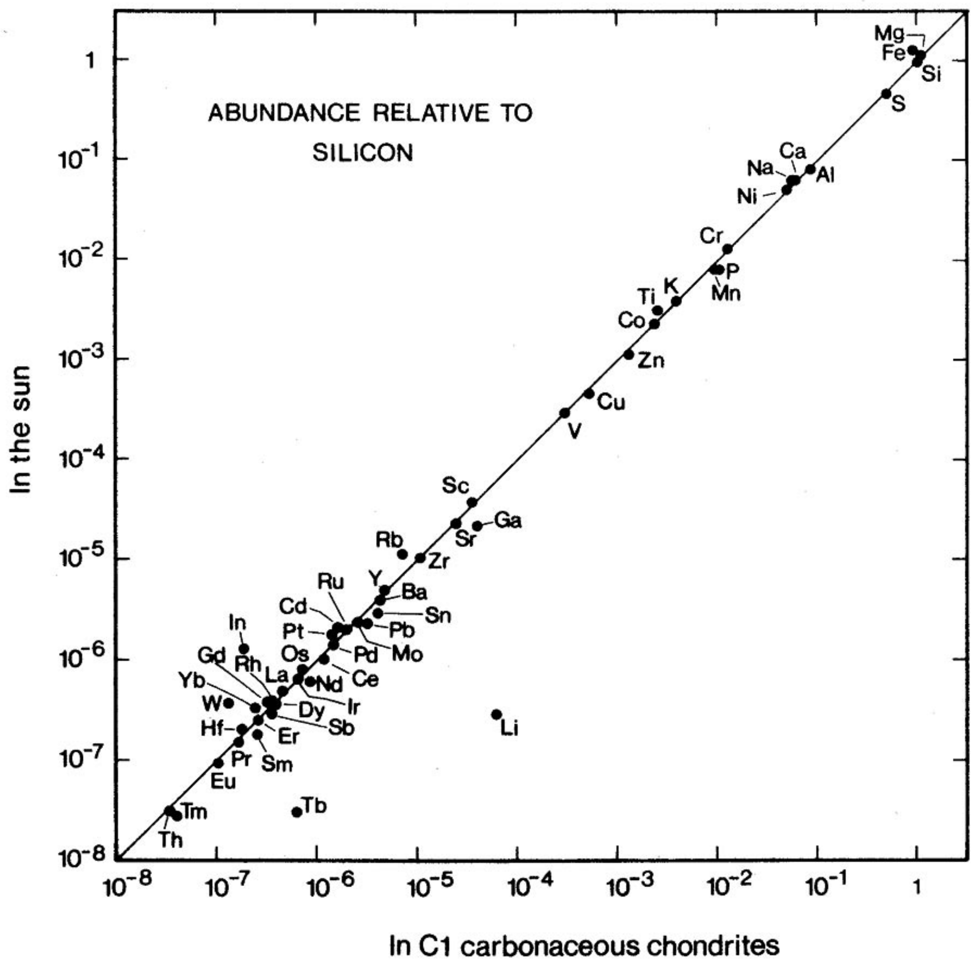

- Comparison of "cosmic abundances" from C1 meteorites vs the Sun

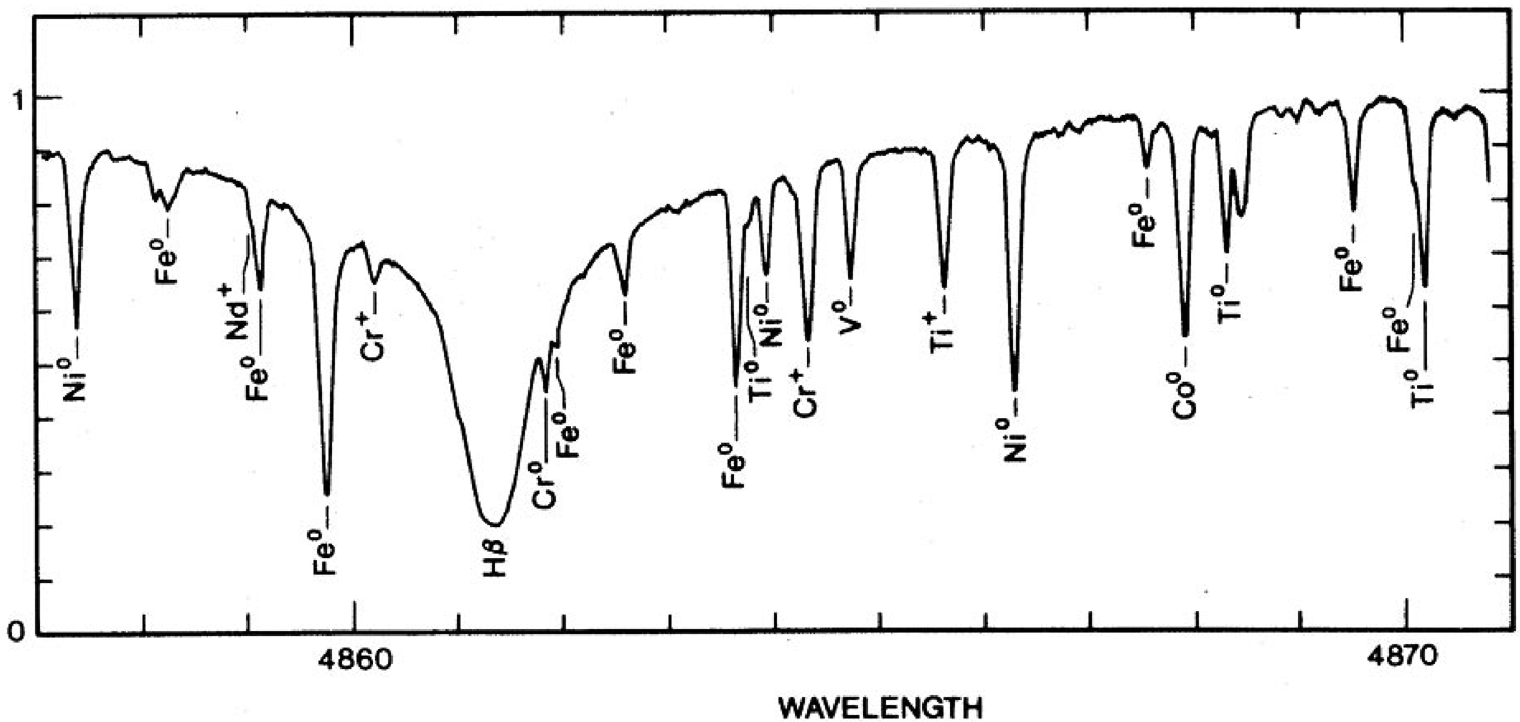

- The chemical composition of the Sun is derived from absorption spectra

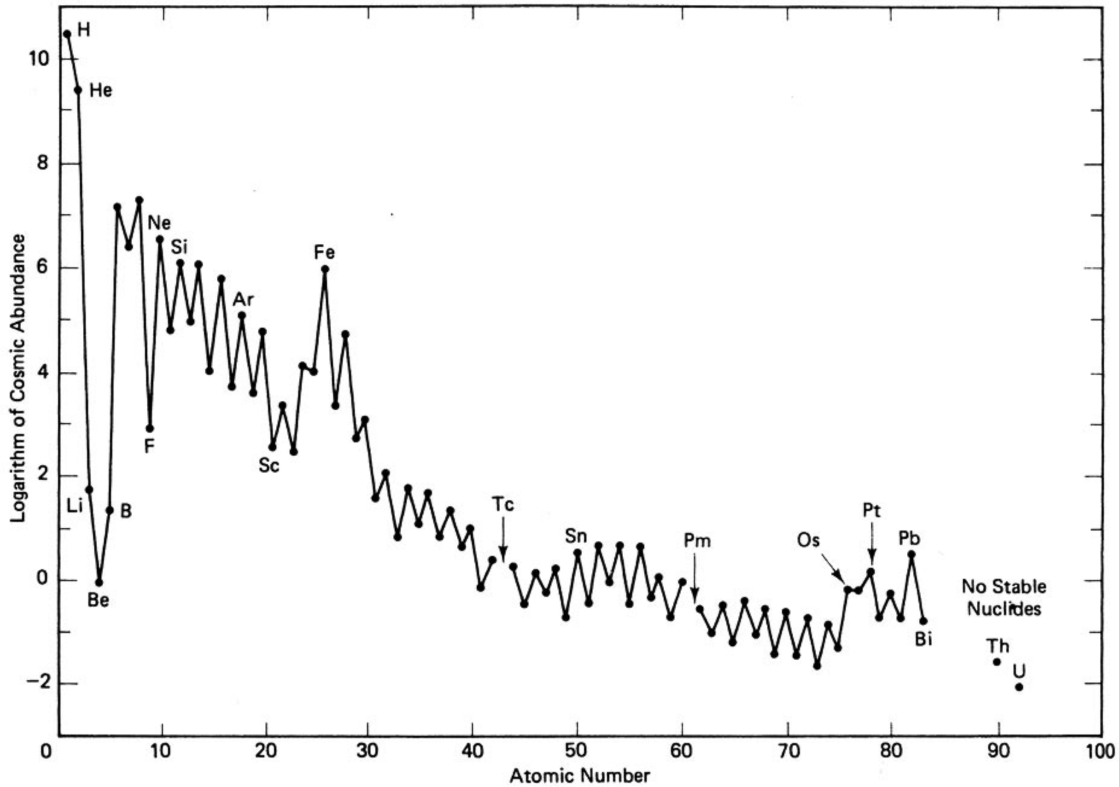

Figure 13.3 Cosmic abundances of the elements, relative to 10^6 silicon atoms.

- Even-Z elements are more abundant than their odd-Z neighbours

- Notice the high relative abundance of the Fe-Ni-group elements

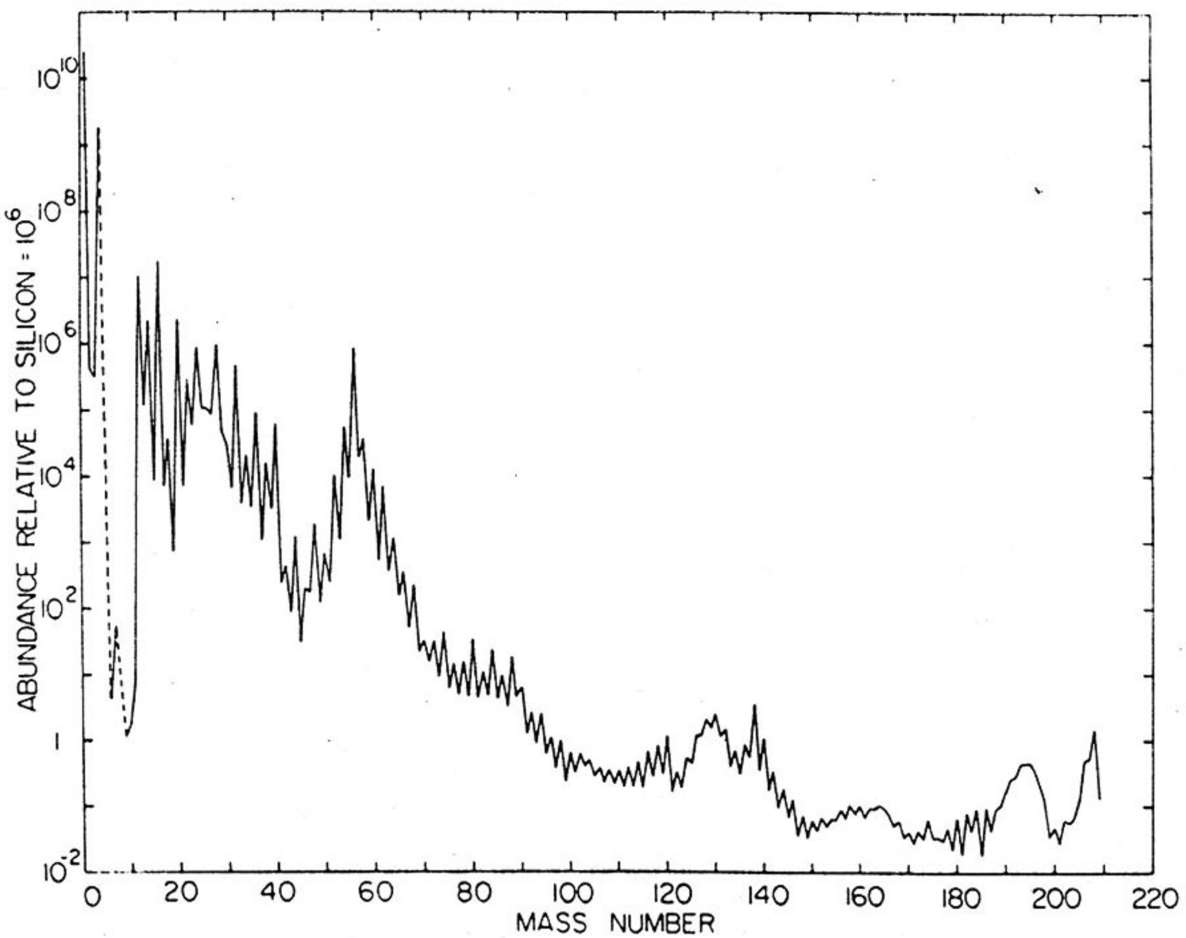

- Odd-Z *vs* even-Z effect is even more pronounced for adjacent nuclides

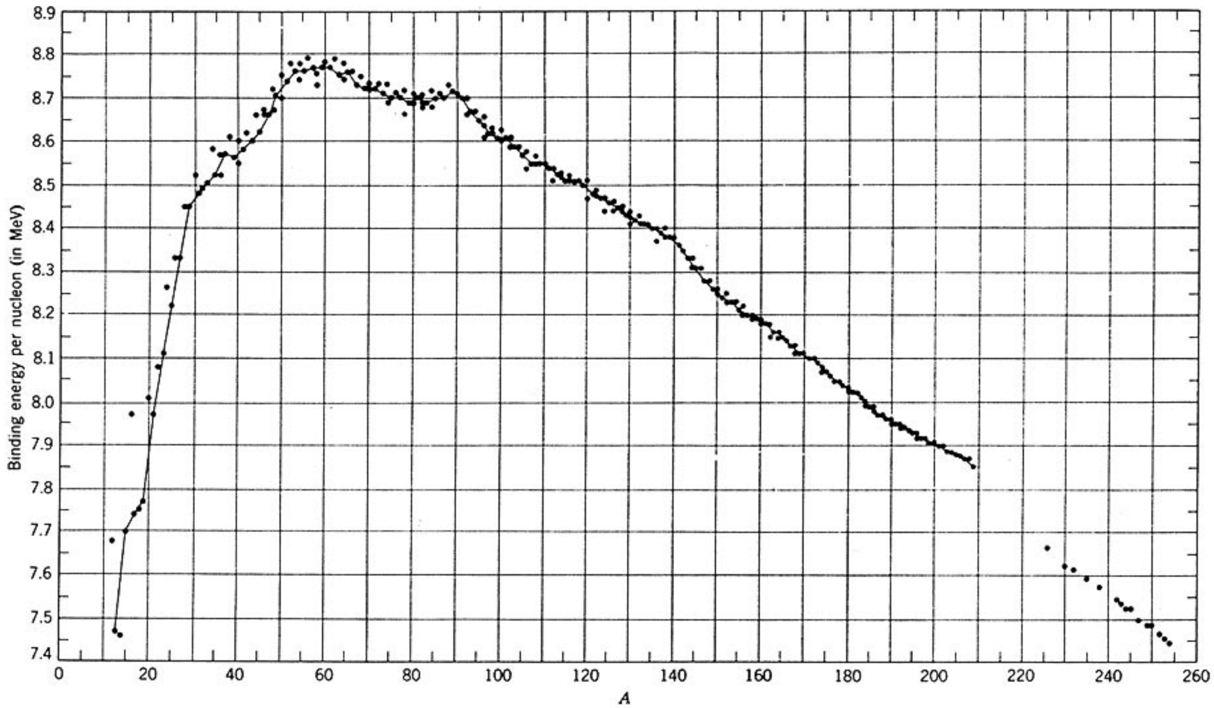

(a)

Fig. 2-1 Average binding energy per nucleon as a function of *A* per stable nuclei. (*a*) $12 \le A \le 250$, with line connecting the odd-*A* points.

- Nuclide abundances follow the rules of nuclear stability - high abundances of Fe-Ni group elements are explained by their high nuclear binding energy.

TABLE 15.1.1
Short-lived Radionuclides in the Early Solar System

Radio-nuclide	Half-life (Myr)	Decay	Daughter	Abundance
		Clear Positive Evidence		
^{146}Sm	103	α	^{142}Nd	$^{146}Sm/^{144}S \sim 0.005$
^{244}Pu	82	α, SF	fission Xe tracks	$^{244}Pu/^{238}U \sim 0.004$–$0.007$
^{129}I	16	β	^{129}Xe	$^{129}I/^{127}I \sim 10^{-4}$
^{107}Pd	7	β	^{107}Ag	$^{107}Pd/^{108}Pd \sim 2 \times 10^{-5}$
^{53}Mn	3.7	β	^{53}Cr	$^{53}Mn/^{55}Mn \sim 4 \times 10^{-5}$
^{26}Al	0.7	β	^{26}Mg	$^{26}Al/^{27}Al \sim 5 \times 10^{-5}$
		Restrictive Upper Limits		
^{247}Cm	16	α	^{235}U	$^{247}Cm/^{235}U < 0.004$
^{41}Ca	0.13	β	^{41}K	$^{41}Ca/^{40}Ca < 10^{-8}$

- Short-lived nuclides (now extinct) were also present in the early solar system.

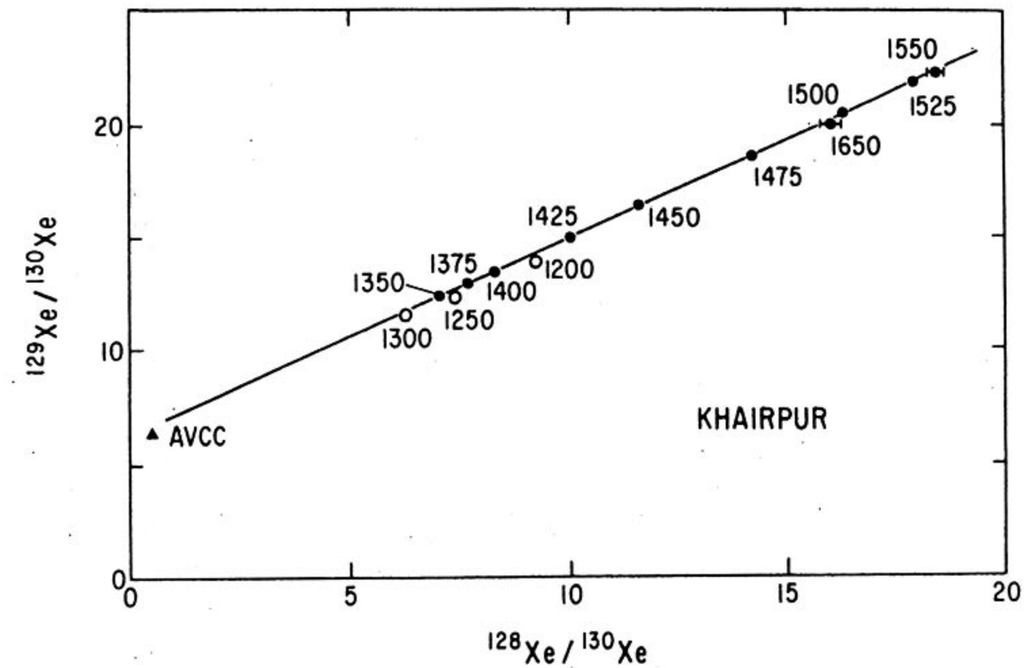

Fig. 15.3.1. Correlation of ^{129}Xe (from decay of ^{129}I) with ^{128}Xe (produced from ^{127}I by neutron irradiation) for the enstatite chondrite Khairpur (figure from Kennedy 1981).

- Xe-129 release from a meteorite correlates with I-derived Xe-128. We infer that Xe-129 is the "fossil" daughter of extinct I-129 ($t_{1/2} = 17$ Myr)

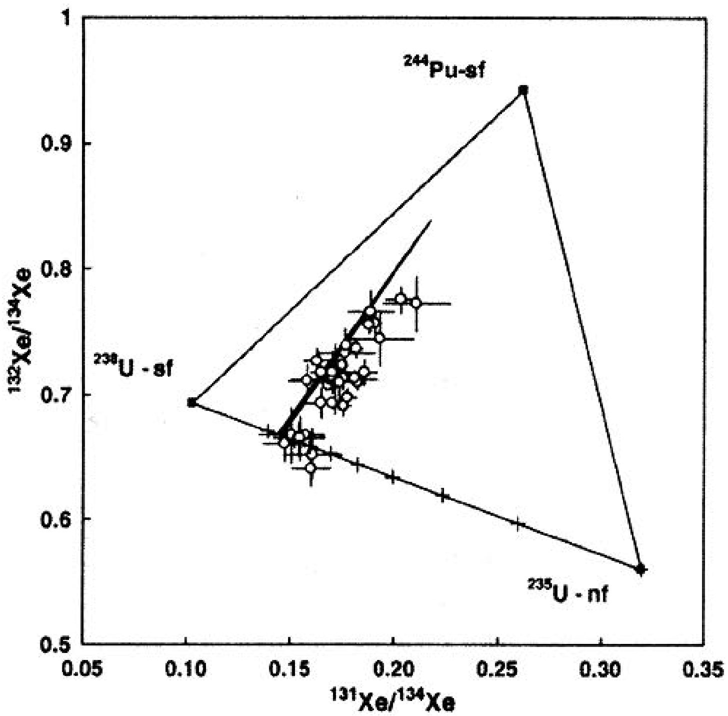

Fig. 1. Air corrected ^{132}Xe/^{134}Xe vs. ^{131}Xe/^{134}Xe ratios. The crosses indicate compositions of uranogenic xenon corresponding to U–Xe ages at 500 Ma intervals, increasing from zero at the ^{235}U end member. The solid lines represent a range of expected xenon compositions for zircons with ages in the range 3976 to 4159 Ma and $(Pu/U)_o$ ratios from zero to 0.016. Position of data points to the right of this line is indicative of xenon loss, a conclusion which is independent of $(Pu/U)_o$.

- Evidence of extinct Pu-244 has also been found in ancient Archean zircons